Molecular Crystals and Liquid Crystals

Publication details, including instructions for authors and subscription information:
http://www.tandfonline.com/loi/gmcl20

Motion of Nonsingular Walls in Plane Layer of Twisted Nematics

V. A. Belyakov [a] & W. Kuczynski [b]

[a] L.D. Landau Institute for Theoretical Physics, Moscow, Russia

[b] Institute of Molecular Physics, Polish Academy of Sciences, Poznan, Poland

Version of record first published: 22 Sep 2010

To cite this article: V. A. Belyakov & W. Kuczynski (2008): Motion of Nonsingular Walls in Plane Layer of Twisted Nematics, Molecular Crystals and Liquid Crystals, 480:1, 243-261

To link to this article: http://dx.doi.org/10.1080/15421400701826688

Mol. Cryst. Liq. Cryst., Vol. 480, pp. 243–261, 2008

ISSN: 1542-1406 print/1563-5287 online
DOI: 10.1080/15421400701826688

Taylor & Francis
Taylor & Francis Group

Motion of Nonsingular Walls in Plane Layer of Twisted Nematics

V. A. Belyakov[1], W. Kuczynski[2]
[1]L.D. Landau Institute for Theoretical Physics, Moscow, Russia
[2]Institute of Molecular Physics, Polish Academy of Sciences, Poznan, Poland

Motion of a nonsingular flat wall in twisted planar nematic layers is investigated for a finite strength of the surface anchoring in the cell. The measurements of the wall velocity as a function of the rotation angle of the cell plate are performed. The theoretical calculations of the corresponding dependences performed for two different model anchoring potentials reveal that for thick samples the both potentials give almost the same results. For thin samples the calculation results for these potentials differ significantly. It is shown that the measurements of the wall velocity allow the determination of the anchoring strength and may be used for the reconstruction of the shape of the actual surface anchoring potential.

Keywords: nematics twisting; nonsingular walls; surface anchoring

INTRODUCTION

The behaviour of the structure of confined chiral liqyid crystals (CLC) with a finite surface anchoring strength under action of continuously changing external agents (temperature, electric or magnetic field etc.) attracts now considerable attention due to the interesting physics of the phenomenon [1,2] and its direct connection to liquid crystal applications [3]. A typical feature of the corresponding behavior is not only smooth changes of the structure in some range of the external agent values but also jump like changes for the definite values of the continuously changing agent and a hysteresis of these jump-like change points if the agent is changed in the opposite direction. For example,

The support of the work by the RFBR grant N 06-02-16287 is greatly appreciated by V.A.B.

Address correspondence to V. A. Belyakov, L.D. Landau Institute for Theoretical Physics, Kosygin str. 2, 117334 Moscow, Russia. E-mail: bel@landau.ac.ru

the jump of the pitch in the cell initiated by a smooth variation of the temperature [1,4,5], electric or magnetic field [6–8] or mechanical rotation of the surface limiting a cell [9] may occur. As it was shown [2,10] for a relatively weak surface anchoring the corresponding jump points and the hysteresis are directly dependent on the shape of the anchoring potential and its strength, so experimental studies of the related phenomena may be useful for the reconstruction of the actual surface anchoring potential. Quite recently another phenomena connected to the shape of the anchoring potential were studied. These are the temporal dynamics of the pitch jump [2,10] and the motion of a non-singular wall dividing the areas of different values of the pitch in a planar CLC layer [11,12]. These studies revealed also the dependence of the temporal evolution of the jump on the shape and the strength of anchoring for a relatively weak surface anchoring. More over, the distribution of director in the non-singular wall (moving or motionless) is also dependent on the shape of surface anchoring potential [12].

All mentioned phenomena are connected with the large angular deviation of the director at the layer surface from the alignment direction. It is why they are suitable for determination of the potential shape. Recall that at the small angular director deviation angles from the alignment direction any surface anchoring potential has to be quadratic on the deviation angle, so the phenomena connected with small director deviation angles from the alignment direction are insensitive to the shape of the surface anchoring potential. As a first step in the direction of restoring of the actual shape of the anchoring potential new model surface anchoring potentials [2,10] were introduced.

It should be noted here that the term "relatively weak surface anchoring" really is related to the large values of the dimensionless parameter $S_d = K_{22}/Wd$, where K_{22} is the elastic twist modulus, d is the layer thickness and W is the depth of the surface anchoring potential. So, at any strength of the anchoring a sufficiently thin layer (small d) insures the conditions of "relatively weak surface anchoring".

We shall study below the phenomenon of the same nature, as mentioned above, occurring when a varying external agent is the orientation of the planar alignment direction at the surface limiting the planar nematic layer. This variation is realized by rotation one of the optical cell plate which results in a twist of the director in the layer and jumps of this twist [9]. If the mentioned jumps happen in a limited area of the layer surface the director distribution over the layer surface become inhomogeneous and a wall, an interface between the configurations with different twist of the director in the layer, occurs.

The wall begins its motion in the direction of the area for which the free energy per a unit layer area is higher than the corresponding value for the second area. However this wall may be motionless. It happens if the free energies of the both area per a unit layer area are the same. Namely, we shall study the motion of a nonsingular flat wall in twisted plane nematic layers for a finite strength of the surface anchoring in the cell at variations of the cell thickness and the cell plate rotation angle.

GENERAL EQUATIONS

Following the approach presented in [9] examine the behavior of the director distribution in a planar nematic layer of finite thickness and finite strength of anchoring at one of its surfaces and infinite at another (see Fig. 1) under rotation of the cell glass plate. At the process under consideration smooth and jump-wise changes of the director field in the layer are possible. We restrict below the analysis of the corresponding variations of the director configuration in the layer by the assumptions that the mechanism of possible jump-wise changes of the director configuration is connected with overcoming by the director of the anchoring barrier at the layer surface.

Following [5,9,13] we write the free energy of the layer in the form

$$F(\varphi_0) = W_s(\varphi) + (K_{22}/2d)(\varphi_0 + \varphi)^2, \quad (1)$$

where $W_s(\varphi)$ is the surface anchoring potential, φ is the angle of deviation of the director orientation at the surface of the layer with finite anchoring from the rotating alignment direction (i.e., the easy direction which is rotated together with the plate), φ_0 is the rotation angle of the cell glass plate (so $\varphi_0 + \varphi$ is the resulting angle of the director twisting over the layer thickness), K_{22} is the twist Frank modulus

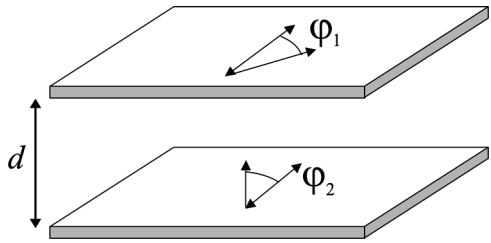

FIGURE 1 Schematic drawing of the layer in the case of unidentical anchoring at the layer surfaces.

and d is the sample thickness. We assume for the definiteness that the initial undistorted state of the nematic cell corresponds to $\varphi = \varphi_0 = 0$.

Under rotation of the cell glass plate, i.e., increasing of φ_0, the modulus of the angle φ (at the beginning of the plate rotation the angle φ is negative) is also smoothly increasing. However for $\varphi_0 > \pi/2$ an abrupt changing of φ may occur (see [9] and the comments on the possible stabilization rotation at $\varphi_0 > \pi/2$ there).

The angle φ may be found from the conditions of minimum of the free energy (1) what gives the following equations for φ:

$$\partial W_s(\varphi)/\partial\varphi + (K_{22}/d)(\varphi + \varphi_0) = 0 \tag{2}$$

The analysis of the Eq. (2) shows that a smooth changing of the director deviation angle φ is possible while the modulus φ is less than some critical angle φ_c. Upon achieving by φ of the critical value φ_c a jump-like change of the pitch occurs and the transition to a new configuration of the director in the layer differing by one in the number of the director half-turns N in the layer occurs. For example, at infinitely strong anchoring at the both surfaces, in our assumption on stability of the planar texture of the cell under rotation of glass plate, the director twist angle (or the number of half-turns N) is just the same as the angle φ_0 and formally may be arbitrary large. At finite strength of anchoring the maximum director twist angle (and consequently, N) is limited by the strength of anchoring. In reality, of course, even at infinitely strong anchoring the maximum director twist angle is also limited and a transition of the system to the ground state with $N \leq 1$ takes place through some mechanism different from the examined here one.

In our case of a finite strength of anchoring at one of the surfaces said above means that it is possible to reach only some finite value of N_c (angle of director twist in the layer) by rotating the cell glass plate. Further rotation of the plate does not allow increasing this limiting value N_c and will result only in a sequence of jump-wise (decreasing) and smooth (increasing) variations of N around N_c.

The value of critical angle in the general case is dependent on the shape of anchoring potential and the anchoring strength at both surfaces [1,5]. So the explicit expressions for φ_c shall be given below for each model potential used in calculations (see Appendix).

The value of the cell glass plate rotation angle at the jump point φ_{0c} is determined by the expression

$$\varphi_{0c} = [\partial W_s(\varphi)/\partial\varphi]_{\varphi=\varphi c}/(K_{22}/d) - \varphi_c. \tag{3}$$

The angle between alignment direction and director just after the jump φ_j is determined by the solution of the following equation

$$\partial W_s(\varphi)/\partial\varphi + (K_{22}/d)[\varphi + \varphi_{0c} - \pi] = 0. \quad (4)$$

As it was shown [1,5] the variations of the pitch in the layer and, in particular, the director twist hysteresis are determined by the dimensionless parameter $S_d = K_{22}/Wd$, where W is the depth of the anchoring potential. This behavior is rather universal because it is not directly dependent on the sample thickness. It means that for every specific form of the anchoring potential the expressions (1–4) may be transformed to the form, which includes the parameters of the problem d, K_{22}, W only in the combination, which reduces to the dimensionless parameter S_d.

At the next section the given above general expressions will be applied to the specific model anchoring potentials.

Infinitely Strong Anchoring at One Surface

Let us apply the given above general expressions to the specific case of infinitely strong anchoring at one of the layer surface and finite anchoring at other surface described by the specific potential $W_s(\varphi)$ (see Appendix). The expressions for the free energy given by Eqs. (1, 2) and others reduce to the following expressions for R-P-potential (A.4 at $n = 1$).

For the free energy one gets from (2):

$$F(T)/W = [-\cos^2\varphi + S_d(\varphi + \varphi_0)^2]/2, \quad (5)$$

where the dimensionless parameter $S_d = K_{22}/Wd$ was already mentioned above.

The angle of director deviation φ from the rotating alignment direction is determined by the following expression

$$\sin 2\varphi + 2S_d(\varphi + \varphi_0) = 0 \quad (6)$$

and the critical angle φ_c is determined by the relationship

$$\cos 2\varphi_c + S_d = 0, \quad (7)$$

i.e. $\varphi_c = [\text{arc}, \cos(-S_d)]/2$.

The Eq. (7) and calculations show that the critical angle φ_c is dependent on the parameter S_d contrary to the case of identical anchoring at the both surfaces [1,5].

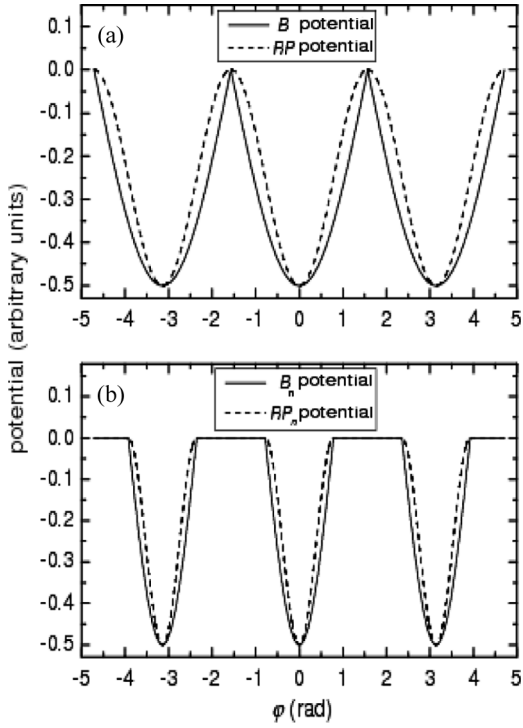

FIGURE 2 Rapini-Papoular (R-P) and B-anchoring potentials and R-P and B-like narrow anchoring potentials.

The value of the cell glass plate rotation angle φ_{0c} corresponding to the jump point is determined from (7) by the following formula

$$\varphi_{0c} = \varphi_c + (\sin 2\varphi_c)/2S_d \tag{8}$$

Solution of Eq. (7) exists only for $S_d < 1$. It means that for weak anchoring (or thin layers) jump-wise changes of director configuration in the layer may be absent. However it should be mentioned that because the Eq. (7) for critical angle was obtained for Rapini-Papoular anchoring model potential the last statement is model dependent. So, experimental investigations of the jump-wise changes of director configuration in the layer may be used for determination of the real shape of the anchoring potential and its deviations from Rapini-Papoular anchoring model potential.

The value of φ_j, i.e., the angle between alignment direction and director just after the jump, is determined by the solution of the

following equation:

$$\ldots \sin 2\varphi_j + 2\ S_d[\varphi_j - [\arccos(-S_d)]/2 + (\sin 2\varphi_c)/2S_d - \pi] = 0, \quad (9)$$

The expressions for the free energy given by Eqs. (1, 2) and following from them formulas reduce to the following expressions for B-potential (A.1).

For the free energy one gets from (2):

$$F(T)/W = [-2\cos^2(\varphi/2) + 1 + S_d(\varphi + \varphi_0)^2]/2. \quad (10)$$

The angle of director deviation φ is determined by the following expressions

$$\sin\varphi + 2S_d(\varphi + \varphi_0) = 0 \quad (11)$$

The critical angle φ_c for B-potential remains to be $\pi/2$ as in the case of identical anchoring at both surfaces.

The value of the cell glass plate rotation angle at the jump point φ_{0c} is determined from (11) by the following formula

$$\varphi_{0c} = \varphi_0(\varphi_c) = \pi/2 + 1/(2S_d) \quad (12)$$

The value of φ_j, i.e. the angle between alignment direction and director just after the jump, is determined by the solution of the following equation:

$$\sin\varphi_j + 2S_d[\varphi_j + 1/(2S_d) - \pi/2] = 0, \quad (13)$$

The given above values of the angles of the director deviation from the rotating alignment direction just before and after the jump and the corresponding value of the cell glass plate rotation angle may be used for the solution of the dynamical problem related to the pitch jump because these values completely determine the initial and final state in the problem to be solved (see [2,10]).

STEADY STATE CALCULATION RESULTS

Below are reproduced the calculation results [9] for the case of infinitely strong anchoring at one of the layer surface and finite anchoring at other surface described by the potential $W_s(\varphi)$ of two shapes, R-P and B-potential (A.4 for $n = 1$ and A.1).

At Figures 3, 4 the director twist angle versus the increasing plate rotation angle is presented. Figures 3, 4 reveal qualitative

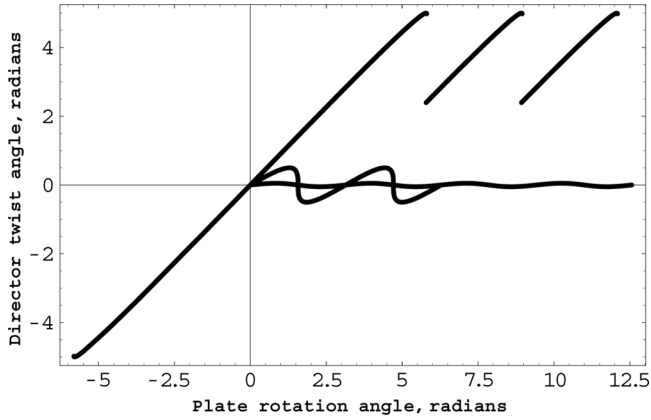

FIGURE 3 Director twist angle versus the plate rotation angle for R-P-potential ($S_d = 0.1,1,10$ (from the top to the bottom)).

difference for these two potentials in the distribution of twisting of the director in the layer caused by the plate rotation. For a strong anchoring (small S_d) the director twist angle versus the plate rotation angle are almost the same for both the R-P and B-potentials. However for a weak anchoring (large S_d) there is a difference between R-P and B-potentials (compare Figs. 3, 4). For the R-P-potential the changes of the director twist angle may be completely smooth for a weak

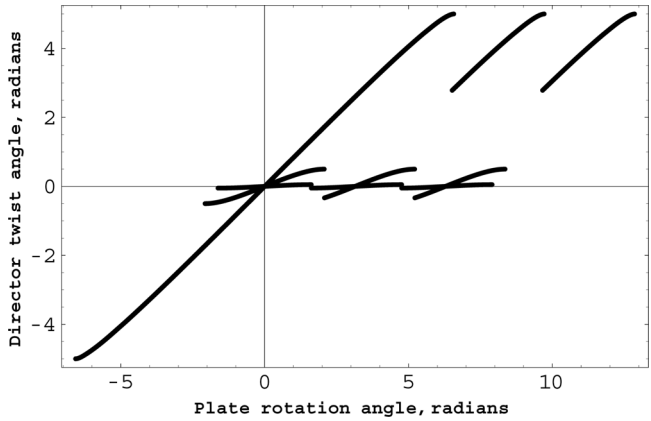

FIGURE 4 Director twist angle versus the plate rotation angle for B-potential ($S_d = 0.1,1,10$ (from the top to the bottom)).

anchoring (large S_d) under the plate rotation at any angle and include jump-wise changes for strong anchoring (small S_d) similar to those ones for B-potential. In the case of B-potential the jump-wise changes of the director twist angle are present at any strength of anchoring while for the R-P-potential at the large $S_d > 1$ the changes of the director twist angle under the plate rotation at any angle are smooth. It means that for B-potential a bistability reveals itself at any strength of anchoring while for the R-P-potential it appears only for a sufficiently strong anchoring.

At the opposite direction of the plate rotation angle the jump points don't coincide with the previous ones and a hysteresis in the curve "the director twist versus the plate rotation" reveals itself (see also [1,5] related to the temperature hysteresis). Figures 3, 4 show also that for the B-potential for any strength of the anchoring and for the R-P-potential for sufficiently strong anchoring ($S_d < 1$) hysteresis of the jump point for opposite direction of the plate rotation exists. If one denotes by φ_{0j}^{+} and φ_{0j}^{-} the plate rotation angle corresponding to the director twist jump for the plate rotation in the initial and the opposite direction, respectively, the corresponding hysteresis in the value of φ_0 is equal to $\varphi_{0j}^{+} - \varphi_{0j}^{-} = 1/S_d$ for B-potential and $\varphi_{0j}^{+} - \varphi_{0j}^{-} = 2\varphi_c + (\sin 2\varphi_c)/S_d - \pi$ for R-P-potential. Becausefor R-P-potential $\pi/4 < \varphi_c < \pi/2$ the hysteresis for it is less than the hysteresis for B-potential at the same S_d and reduces to zero for $S_d = 1$. The absence of the hysteresis for R-P-potential at weak anchoring ($S_d > 1$) constitutes a qualitative difference between R-P and B-potentials.

As one sees from the Figures 3, 4 the jumps of the director twist angles result in a new homogeneous configuration of the director in the layer. However if the jump occurs in the limited area of the cell surface a wall may arise between the areas of different director twist in the layer. The wall begins its motion in the direction of the area for which the free energy per a unit layer area is higher than the corresponding value for the second area. However this wall may be motionless. It happens if the free energies of the both area per a unit layer area are the same. It corresponds to the plate rotation angle to be equal to $\pi/2$.

The jumps points at Figures 3, 4 happen at $\varphi = \varphi_c$ and corresponds to the maximal difference of the free energies, i.e. to the maximal velocity of the wall. But if the plate rotation angle is reduced to $\pi/2$ the wall will stop. If the plate rotation angle φ_0 satisfies to the condition $\pi/2 < \varphi_0 < \varphi_{0c}$ the velocity of the wall is between zero and its maximal value corresponding to φ_{0c}. So, there is a simple way to change the wall velocity by rotating a cell plate and consequently a problem arise to find the wall velocity as a function the plate rotation angle.

Motion of a Flat Wall

The wall between the area of a planar nematic layer with differing twisting of the director at the layer thickness and its motion are very similar to the corresponding problem for a cholesteric planar layer studied recently in [12]. It is why we shall use the main results of the cited paper with needed modifications omitting the details which may be found in [12]. Like in [12] we shall consider a non-singular flat wall moving at a constant velocity v_s in the direction perpendicular to the wall.

The velocity v_s is determined by the condition of equality of the viscose energy dissipation rate to the rate of the energy release due to the transition from the twisted configuration of a higher free energy (per a unit area) to the configuration of a lower free energy. It is dependent on the difference of the free energies of the layer (per a unit area) for these configurations, distribution of the director in the wall, the rotational viscosity of the nematic γ_1, and is determined by the expression [11,12]:

$$v_s = -\Delta F/(\gamma_1 V), \tag{14}$$

where ΔF is the difference of the free energies of the layer (per a unit area) for the twist configurations under the consideration dependent on the plate rotation angle φ_0 and V is the dependent on the wall structure dissipation integral determined by the following formula:

$$V = \int (d\o(x,z)/dx)^2 dzdx, \tag{15}$$

where the integration is carried out all over the layer volume, $\o(x,z)$ is the local (dependent on the coordinate x along the wall motion and coordinate z detrmining the distance from the the layer surface) director twist angle. One can calculate exactly the first factor ΔF in the right side of Eq. (14) using Eq. (1) for the free energy of the layer as a function of at φ_0. An exact calculation of the dissipation integral assumes the knowledge of the director distribution in the wall. Generally speaking the director distribution in the wall is dependent on the wall velocity v_s, however following [12] we shall neglect by the difference of the moving and motionless wall shape in the calculations of the wall velocity v_s and shall exploit the results on the motionless walls obtained in [12].

It was shown [12] that a dimensionless motionless wall shape presented as the director twist angle divided by the angular jump versus the coordinate x divided by the wall thickness is almost independent on the parameters of the problem. So, in the direct analogy with

[14,15] (see also Chapter 3 in ref. [16a]) one gets the following approximate analytical expression for $\varphi_s = \pi/2 - \varphi$ [12] (i.e., for the director twist angle relative to the surface director orientation at the centre of the wall).

$$\varphi_s/(\pi/2 - \varphi_e) = \pm\{1 - (4/\pi)\text{arctg}[\exp(-|x|/L)]\}, \tag{16}$$

where $\pi - 2\varphi_e$ is the angular jump at the wall and L is the wall thickness and in (16) the opposite signs have to be used at the opposite sides of the wall.

Under our assumption on coincidence of the shapes of moving and motionless wall one gets with the help of (16) the following expression for the entering in (14) dissipation integral (15)

$$V = (1 - 2\varphi_e/\pi)^2(2d/3L). \tag{17}$$

It is convenient to present the variations of wall velocity v_s versus the plate rotation angle φ_0 normalized by the velocity at some characteristic twist (for example at the twist angle of absolute instability, i.e., at $\varphi_0 = \varphi_{0c}$ (see Figs. 3, 4):

$$v_s(\varphi_0)/v_s(\varphi_{0c}) = [\Delta F(\varphi_0)/\Delta F(\varphi_{0c})][V(\varphi_{0c})/V(\varphi_0)], \tag{18}$$

where $V(\varphi_0)$ is the dependent on the plate rotation angle φ_0 dissipation integral determined by the Eq. (15). One can calculate exactly the first factor in the right side of Eq. (18) using Eq. (1) for the free energy of the layer as a function of φ_0. What is concerned of the second factor in the right side of Eq. (18) it may be calculated relatively simple if one accepts the discussed above approximation of the independence of the wall shape on the wall velocity. Under this assumption the dissipation integral is given by the expressions (17) where the factor $\pi(1 - 2\varphi_e/\pi)$, i.e., the angular jump of the director at the wall for a motionless wall, has to be changed by the angular jump $\Delta\varphi(\varphi_0)$ for a moving wall dependent on the plate rotation angle φ_0. $\Delta\varphi(\varphi_0)$ has to be calculated on the base of the free energy (1) and may be presented as a function of φ_0. Finally expression (18) reduces to:

$$v_s(\varphi_0)/v_s(\varphi_{0c}) = [\Delta F(\varphi_0)/\Delta F(\varphi_{0c})][\Delta\varphi(\varphi_{0c})/\Delta\varphi(\varphi_0)]^2[L(\varphi_0)/L(\varphi_{0c})]. \tag{19}$$

As a first approximation one may assume that the wall width L in (19) is independent on the plate rotation angle φ_0.

It is useful to present here a simple formula for $v_s(\varphi_0)$ to which Eq. (14) reduces if the wall is almost a motionless one, i.e., if the director deviation angle from the alignment direction at the surface

φ is very close to the corresponding director deviation angle φ_e for a motionless wall what just corresponds for the plate rotation angle φ_0 being close to $\pi/2$. In this limit one using Eqs. (1, 2) easily finds that Eq. (14) reduces to

$$v_s = 2(\varphi_0 - \pi/2)(\partial W_s(\varphi)/\partial\varphi)_{\varphi=\varphi e}/(\gamma_1 V) \tag{20}$$

which shows that for φ_0 close to $\pi/2$ the velocity v_s is linearly dependent on the plate rotation angle.

The relationship (20) may be useful for the experimental restoration of the actual surface anchoring potential. Really, the measured wall velocity is proportional (with a known proportionality factor) to the derivative of the surface anchoring potential at the angle $\varphi = \varphi_e$. It means that one can restore experimentally the derivative of the surface anchoring potential in sufficiently wide angular interval of $\varphi$by varying φ_e (the last may be done, for example, by varying the sample thickness). The calculations of φ_e as a function of the layer thickness and the parameter S_d for the model R-P and B- potentials may be found in [9] (see Figs. 5, 6 in [9]).

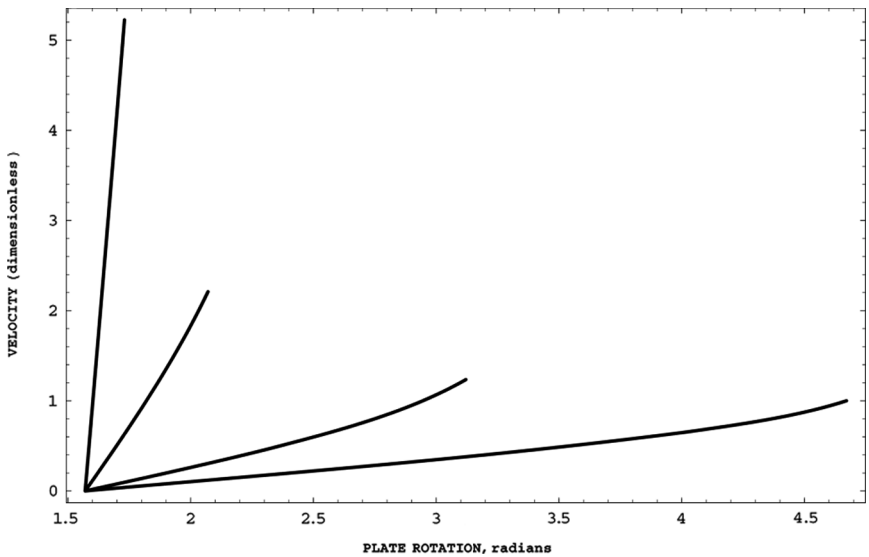

FIGURE 5 Calculated flat wall velocity versus the plate rotation angle for B-potential at $S_d = 1/2\pi$, $1/\pi$, 1, 3 (from the bottom to the top) normalized by velocity at the critical free rotation angle for $S_d = 1/2\pi$).

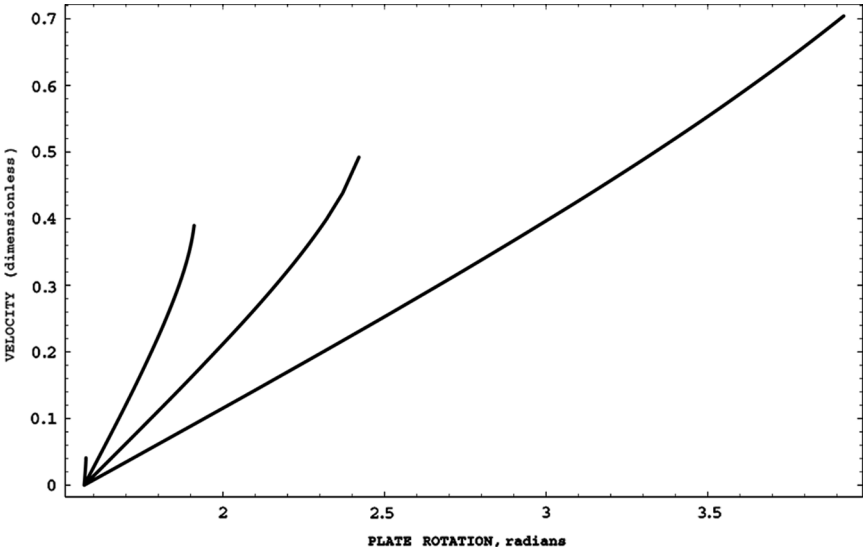

FIGURE 6 Calculated flat wall velocity versus the plate rotation angle, for R-P-potential at $S_d = 1/2\pi$, $1/\pi$, 0.5, 0.95 (from the bottom to the top) normalized by velocity at the critical plate rotation angle for $S_d = 1/2\pi$ for B-potential.

CALCULATION RESULTS ON THE WALL MOTION

The calculated dependences of the wall dimensionless velocity, i.e., $v_s(\varphi_0)/v_s(\varphi_{0c})$, on the plate rotation angle for the R-P- and B-potentials (see Appendix) under the simplifying assumption that the wall width does not depend on the plate rotation angle, i.e., $[L(\varphi_0)/L(\varphi_{0c})] \equiv 1$ in Eq. (19), are presented at Figures 5, 6. The calculated at Figures 5, 6 dependences of the flat wall velocity on the plate rotation angle reveal essential difference for the R-P- and B-potentials. The qualitative difference is in the fact that for the B-potential a moving (as well as a motionless) wall exists at any value of the parameter S_d and for the R-P-potential a moving (as well as a motionless) wall exists if only $S_d < 1$. What is concerned of the quantitative side, as the Figures 5, 6 show, the velocity of a flat wall for the same value of S_d is significantly higher for the B-potential. This correlates with the temperature dependences of the non-singular walls in cholesterics [12]. The dependencies of the flat wall velocity in cholesterics on the layer thickness and the parameter S_d, as the calculations performed in [11] demonstrate, are also quite different for the R-P- and B-potentials. What is concerned of the absolute value of the maximal flat wall velocity

$v_s(\varphi_{0c}) \equiv v_s(\varphi_c)$ (see [11,12]), for the B-potential at the layer thickness $d = 5\,\mu m$, typical values of K_{22}, γ_1 [16] and $S_d \approx 1/2$ it occurs to be $\approx 2\,mm/s$ and 10–15 times less for the R-P-potential decreasing with growth of the layer thickness for the both model potentials (the natural scale of the wall velocity is $K_{22}/d\gamma_1 \approx 0.1\,mm/s$ for the same parameters of the layer). It means that the experimental investigations of a flat wall motion may be used to distinguish possible different shapes of the surface anchoring potential.

EXPERIMENTAL

We prepared the measuring cell consisted of two carefully cleaned glass plates. Both plates were unidirectional rubbed. This procedure

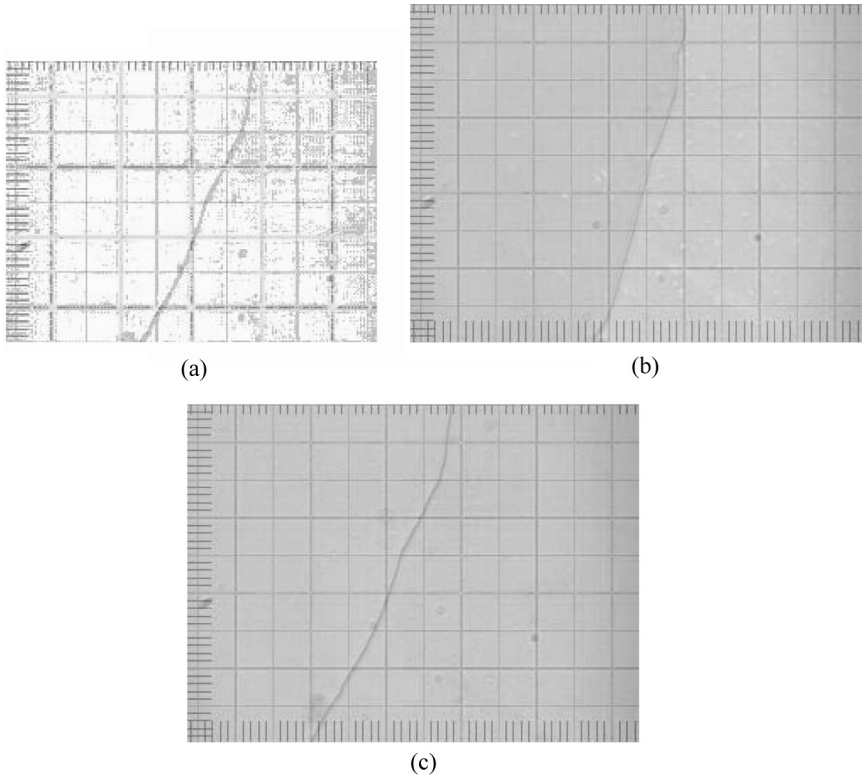

FIGURE 7 The wall observed under polarizing microscope (the long edge of the photograph is 600 microns) at the layer thickness $d = 4.4\,\mu m$, (a) motionless wall (plate rotation angle $\varphi_0 = 90^\circ$), (b) plate rotation angle $\varphi_0 = 170^\circ$, (c) motionless wall (plate rotation angle $\varphi_0 = 270^\circ$).

secured a homogeneous, planar orientation of the nematic layer. One plate was gently rubbed on a velvet patch, and the other–using a buffing machine. Gentle rubbing gave rather weak anchoring. The experiments were performed with the liquid crystal 1-(trans-4-hexyloxycyclohexyl)-4-isothiocyanatobenzene (abbreviated 6CHBT here). The nematic phase in this material has a large temperature range, including room temperature (from 12°C up to 42°C). The nematic liquid crystal 6CHBT was introduced between the plates arranged with the rubbing directions parallel and the sample was placed on the microscope stage between crossed polarizers. The bottom plate prepared for rather weak anchoring was fixed to the stage. The upper plate prepared to get strong anchoring was fixed to the microscope objective. Then, the microscope stage was turned by an angle φ from the range 90–180 degrees causing the twisting of the nematic director within the sample. After some time ranging from seconds to minutes (depending on the value of φ) a wall separating areas with director twist differing by 180 degree was created. To diminish the elastic energy, the area with smaller twist was growing at the expense of the area with larger twist, so the wall was moving. After a while, the line adopted the straight shape and moved with a constant velocity. Typical examples of the wall, as observed under polarizing microscope, are shown in Figure 7.

The movement of the wall was registered with a digital camera attached to the microscope and stored in the personal computer.

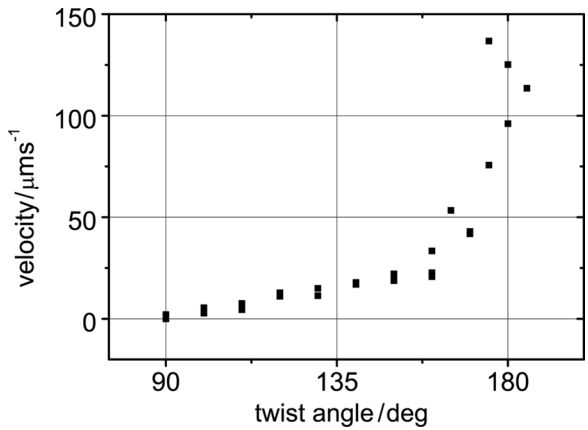

FIGURE 8 Measured flat wall velocity versus the plate rotation angle (at the layer thickness d = 4.4 μm).

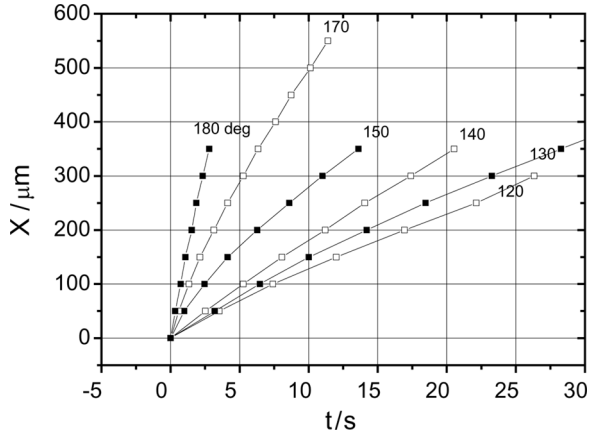

FIGURE 9 Measured distance covered by a flat wall versus the time for several plate rotation angles (at the layer thickness $d = 4.4\,\mu m$).

The registration speed was 15 frames/second. The records were analyzed after splitting the file into individual pictures.

In the limit of small deviations of the plate rotation angle from $\pi/2$ (the rotation angle corresponding to a motionless wall) the wall velocity was a linear function of the plate rotation angle (see Fig. 8), as the theory predicts according Eq. (20).

The analysis demonstrated that in agreement with Eq. (14) the straight walls were moving with a constant velocity. Example are shown in Figure 9.

CONCLUSION

The presented above results show that the variations of a flat wall velocity under rotation of the easy direction in a plane nematic layers with a finite strength of surface anchoring (as well as the temperature variations of a flat wall velocity in plane cholesteric layers with a finite strength of surface anchoring [11,12] and the dynamics of pitch jump in the same layers [2,9,10]) are directly dependent on the shape and the strength (dimensionless parameter S_d) of anchoring potential. It is why the studies of these phenomena allow one in the simplest case to determine anchoring strength and in general case not only to determine the anchoring strength but also to reconstruct the shape of anchoring potential. In particular, these results may be considered also as a starting point for studying of the dynamics of the director

configuration transformations at finite surface anchoring. Note, that the difference of the anchoring potentials reveals itself in a full strength if the surface anchoring is sufficiently weak. The recent advance in obtaining low surface anchoring energy [17,18] allows to hope that the reconstruction of the anchoring potential shape is a quite solvable experimental problem. What is concerned of the results of the present study they demonstrate a qualitative agreement of the theory and experiment and show that for a quantitive comparison of the theory and experiment further experimental studies have to be performed.

There is another aspect of the problem not touched here. One also has to keep in the mind that a nonsingular wall dividing the areas of different director twist may exist for sufficiently thin layers only [12] and above some critical thickness of the layer it has to be substituted by a defect line in the director distribution. So, the obtained above expressions for the wall velocity as a function of the plate rotation angle "work" for the layer thicknesses below the mentioned critical thickness only. It is why if one experimentally finds the point (thickness), for which the above expressions for the wall velocity failed to "work", it opens a new way to estimate the defect line energy. Just at this thickness the nonsingular wall energy becomes equal to the defect line energy the precise knowledge of which is rather vague [16,19,20]. So, along with the mentioned way to restore the actual surface anchoring potential by measuring the wall velocity the studies of the wall velocity dependence on the layer thickness for determining the linear defect energy may be regarded as a quite urgent experimental problem in the physics of liquid crystals.

APPENDIX

New Model Surface Anchoring Potentials

For the purpose of easy reference we give below expressions for the Rapini-Papoular (R-P), so called, B-potential recently introduced in [2], and the narrow angular width R-P-like and B-like model surface anchoring potentials introduced in [10,11] (see Fig. 2).

The B-potential [2] is given by the formula:

$$W_s(\varphi) = -W[\cos^2(\varphi/2) - 1/2], \quad \text{if } -\pi/2 < \varphi < \pi/2. \tag{A.1}$$

The period of the B-potential is π, i.e., $W_s(\varphi + \pi) = W_s(\varphi)$.

The narrow B_n-potential ($n > 1$):

$$\begin{aligned} W_s(\varphi) &= -W(\cos^2(n\varphi/2) - 1/2), \quad \text{if } -\pi/2 < \varphi < \pi/2n, \\ W_s(\varphi) &= 0, \qquad\qquad\qquad\qquad\quad \text{if } \pi/2n < |\varphi| < \pi/2, \end{aligned} \tag{A.2}$$

and continued periodically to $|\varphi| > \pi/2$ (see Fig. 2), according to the relation $W_s(\varphi) = W_s(\varphi - \pi)$, where $n > 1$ ($n = 1$ corresponds to the B-potential).

The free energy (1) for the B_n-potential accepts the following form:

$$\begin{aligned} F(T)/W &= -(\cos^2(n\varphi/2), -1/2) + (S_d/2)[\varphi - \varphi_0(T)]^2 \\ &\quad \text{if } -\pi/2n < \varphi < \pi/2n, \\ F(T)/W &= (S_d/2)[\varphi - \varphi_0(T)]^2 \\ &\quad \text{if } \pi/2n < |\varphi| < \pi - \pi/2n. \end{aligned} \tag{A.3}$$

By a similar way, as B_n-potential, is determined the narrow R-P_n-potential:

$$\begin{aligned} W_s(\varphi) &= -(W/2)(\cos^2(n\varphi), \quad \text{if } -\pi/2n < \varphi < \pi/2n, \\ W_s(\varphi) &= 0, \qquad\qquad\quad \text{if } \pi/2n < |\varphi| < \pi/2, \end{aligned} \tag{A.4}$$

and continued periodically to $|\varphi| > \pi/2$ (see Fig. 2), according to the relation $W_s(\varphi) = W_s(\varphi - \pi)$, where $n > 1$ ($n = 1$ corresponds to the R-P-potential).

The free energy (1) for the R-P_n-potential accepts the following form:

$$\begin{aligned} F(T)/W &= [-\cos^2(n\varphi) + S_d[\varphi - \varphi_0(T)]^2]1/2, \quad \text{if } -\pi/2n < \varphi < \pi/2n, \\ F(T)/W &= (S_d/2)[\varphi - \varphi_0(T)]^2, \qquad\qquad\qquad\quad \text{if } \pi/2n < |\varphi| < \pi - \pi/2n. \end{aligned} \tag{A.5}$$

One has to keep in the mind that the B-potential, being an alternative to the R-P-potential, is some simple and convenient idealization of the physically acceptable surface anchoring potential. Namely, the B-potential has a discontinuous first derivative at the maximum point (edge of the potential well) and thus the curvature is infinitely large. However, one should accept it as a simple model for a class of possible potentials with a very sharp maximum (i.e. very large but finite curvature at the well edge). What is concerned of the R-P-like and B-like surface anchoring potentials with a narrow angular potential well they are natural generalizations of

the R-P- and B-potentials which may be useful in the case of a liquid crystal limited, for example, by a single crystal. In this case more than one alignment direction exists, so the widths of anchoring potential well corresponding to each alignment direction have to be less than π. If one alignment direction is much "stronger" than all other ones, it is possible in the first approximation to neglect by all surface anchoring wells except the one related to the "strong alignment direction." As a result one obtains the potential of R-P_n- and B_n-type discussed here.

REFERENCES

[1] Belyakov, V. A., Oswald, P., & Kats, E. I. (2003). *JETP*, *96*, 915.
[2] Belyakov, V. A., Stewart, I. W., & Osipov, M. A. (2004). *JETP*, *90*, 73.
[3] Kim, J., Yoneya, M., & Yokoyama, H. (2002). *Nature*, *420*(6912), 159.
[4] Zink, H. & Belyakov, V. A. (1996). *MCLC*, 265, 445 (1995); *JETP Letters*, *63*, 43.
[5] Belyakov, V. A. & Kats, E. I. (2000). *JETP*, *91*, 488.
[6] Belyakov, V. A. & Kats, E. I. (2001). *JETP*, *93*, 380.
[7] Belyakov, V. A. (2002). *JETP Letters*, *76*, 88.
[8] Belyakov, V. A. & Semenov, S. V. (2005). Proceedings of SPIE, Vol. 6023 (*SPIE*, *Bellingham*, *WA*) 6023-08.
[9] Belyakov, V. A. & Kuczynski, W. (2005). *MCLC*, *265*, 445.
[10] Belyakov, V. A., Stewart, I. W., & Osipov, M. A. (2005). *Phys. Rev. E*, *71*, 051708.
[11] Belyakov, V. A., Oswald, P., & Kats, E. I. (to be published).
[12] Belyakov, V. A., Osipov, M. A., & Stewart, I. W. (2006). *J.Phys.: Condens. Matter*, *18*, 4443.
[13] Zink, H. & Belyakov, V. A. (1997). *JETP*, *85*, 488.
[14] Pindak, R., Young, C. Y., Meyer, R. B., & Clark, N. A. (1980). *Phys. Rev. Lett.*, *45*, 1193.
[15] Dolganov, P. V. & Bolotin, B. M. (2003). *Pis'ma v ZhETF*, *77*, 503 (2003); (*JETP Letters*, *77*, 429.
[16] a) de Gennes, P. G. & Prost, J. (1993). *The Physics of Liquid Crystals*, Clarendon Press: Oxford; (b) Oswald, P. & Pieranski, P. (2000). Les cristaux liquides: concepts et propriétés physiques illustrées par des expériences. Gordon and Breach Science Publishers: Paris.
[17] Pamdane, O. Ou., Auroy, Ph., Forget, S. et al. (2000). *Phys. Rev. Lett.*, *84*, 3871.
[18] Reznikov, Yu. et al. *SPIE* (to be published).
[19] Smalyukh, I. I. & Lavrentovich, O. D. (2002). *Phys. Rev. E*, *66*, 051703.
[20] Smalyukh, I. I. & Lavrentovich, O. D. (2003). *Phys. Rev. Lett.*, *90*, 085503.